Suppression Efficiency of the Correlated Noise and Drift of Self-oscillating Pseudo-differential Eddy Current Displacement Sensor

Chaturvedi, V.; Vogel, J.G.; Nihtianov, S.

DOI
10.1016/j.proeng.2016.11.312

Publication date
2016

Document Version
Final published version

Published in
Procedia Engineering

Citation (APA)
Chaturvedi, V., Vogel, J. G., & Nihtianov, S. (2016). Suppression Efficiency of the Correlated Noise and Drift of Self-oscillating Pseudo-differential Eddy Current Displacement Sensor. *Procedia Engineering*, *168*, 946-949. https://doi.org/10.1016/j.proeng.2016.11.312

Available online at www.sciencedirect.com

ScienceDirect

Procedia Engineering 168 (2016) 946 – 949

Procedia Engineering

www.elsevier.com/locate/procedia

30th Eurosensors Conference, EUROSENSORS 2016

Suppression Efficiency of the Correlated-noise and Drift of Self-oscillating Pseudo-differential Eddy Current Displacement Sensor

Vikram Chaturvedi, Johan Vogel, Stoyan Nihtianov

Electronic Instrumentation Labartory, Delft University of Technology, Delft, The Netherlands

Abstract

The suppression efficiency of the correlated noise and drift of self-oscillating front-end circuit in a pseudo-differential eddy-current displacement sensor (ECDS) is investigated using COMSOL and MATLAB. The transfer characteristic of the sensor coil, excited at 200 MHz, is obtained through a FE model in COMSOL. The characteristic is linearized to a second-order fit around a standoff distance to the target (x_{so}) of 55 μm. The nonlinearity of the interface is modelled in MATLAB. It is found that, in order to tolerate 1 % drift in the oscillator amplitude, a maximum 2nd harmonic distortion (HD2) of the interface has to be less than −72 dB when the sensor HD2 is −51.5 dB for 5 μm displacement range around x_{so} = 55 μm.

Peer-review under responsibility of the organizing committee of the 30th Eurosensors Conference

Keywords: displacement, sensor, eddy-current, demodulator, oscillator, drift, nonlinearity, finite element

1. Introduction

Precise displacement sensing is one of the very essential requirements in various industries as hi-tech industry, metrology, nano-mechatronics and space-equipment manufacturing [1]. Displacement sensors can also be used for measuring other physical quantities, which can first be converted into movement, such as pressure, acceleration, etc. This can enable us in building pressure sensors, accelerometers, vibrometers etc. [2,3].

Eddy-current displacement sensors (ECDS) are compact, robust, stable, accurate and relatively low-cost. One advantage of ECDSs is that they are quite immune to environmental conditions and are not sensitive to the presence of contaminants as oil, dirt, dust etc. However, ECDS are sensitive to stray magnetic fields, mechanical instability of the sensor coil, etc. Precise displacement measurement with ECDSs is possible only with conductive (metallic) targets, or non-conductive targets with a conductive film on them. An important factor in the performance of the ECDS is the skin-effect. To reduce its impact on the resolution, higher excitation frequency has to be used [4-6].

Peer-review under responsibility of the organizing committee of the 30th Eurosensors Conference
doi:10.1016/j.proeng.2016.11.312

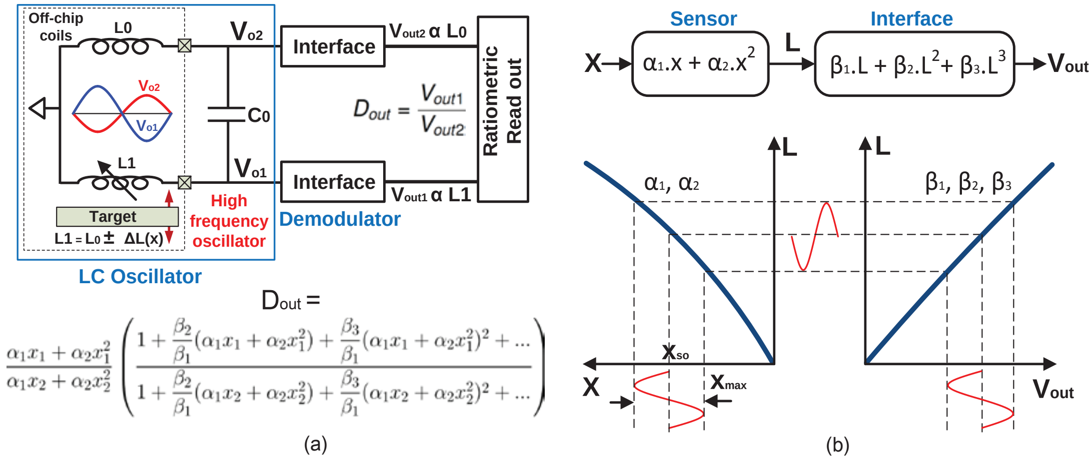

Fig. 1. A pseudo-differential self-oscillating ECDS interface. (a) Voltages across reference coil L_0 and sensor coil L_1 are amplitude-demodulated by the interface. (b) Displacement X goes through nonlinear transfer characteristics of the sensor and the interface.

Figure 1(a) illustrates the conceptual block diagram of a pseudo-differential self-oscillating eddy-current displacement sensor (ECDS) interface. The front-end comprises a LC oscillator which has two coils: (a) Sensor coil L_1 which induces eddy-currents in the metallic target via its time-varying magnetic field. (b) Reference coil L_0 which is shielded from the target and nominally has inductance equal to that of the sensor coil at the standoff distance (x_{so}). For simplicity, the –R (-gm) block needed to sustain the oscillations in the high-frequency oscillator is not shown. Eddy-currents induced in the target produce a secondary magnetic field that changes the inductance of the sensor coil ($L_1 = L_0 \pm \Delta L(x)$). The level of change of the inductance (ΔL) depends on the distance between the sensor coil and the target, and is detected by the demodulation circuit (Interface).

Oscillator outputs V_{o1} and V_{o2} are amplitude-demodulated to baseband voltages V_{out1} and V_{out2}, respectively. These voltages are then digitized and a ratio-metric readout (D_{out}) is performed to suppress the correlated noise and drift of the front-end circuitry [4,5]. Ratio-metric measurement is indispensable for a high precision and highly stable ECDS interface. However, the efficiency of the suppression is limited by the nonlinearity of the interface. Fig. 1(b) shows that due to nonlinearity of the sensor transfer function and that of the interface, the displacement x undergoes two nonlinear transfer functions. Hence it is important to evaluate the minimum linearity required from the interface for a given sensor characteristics and drift budget.

2. Models for sensor and interface

This section discusses the models used for the sensor coil and the interface. The sensor coil transfer characteristics is deduced using COMSOL and the interface behavior is modelled in MATLAB.

2.1. Sensor coil FE model

Figure 2(a) shows the flat Archimedean coil that was used in this analysis. The 6 turn coil had an outer radius of 3 mm and a trace width and an inter-trace distance of 0.1 mm. The thickness of the coil was 30 µm. The coil's standoff from the copper target was 55 µm. The sensor characteristic $L(x)$ was obtained using an axis-symmetric FE model in COMSOL's Magnetic Fields interface. Figure 2(b) shows the magnetic field magnitude in a cross-section close to the coil windings. The coil's inductance depends on the magnetic field magnitude and is, as such, a measure for the coil's standoff from the target.

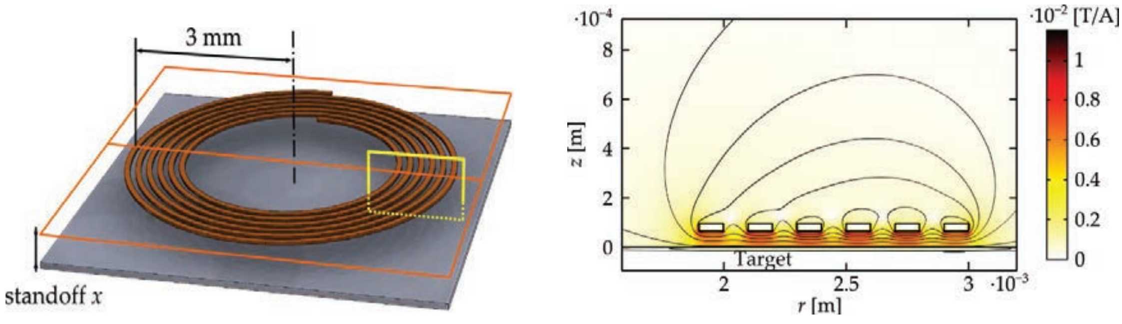

(a) (b)

Fig. 2. Illustration of the coil that was used in this analysis. (a) coil structure. (b) Magnetic field magnitude in a cross-section close the coil windings (indicated in yellow in Fig. 2(a)).

To obtain precise simulation results (a precision in the order of 10^{-14} H, corresponding to 20 pm), a fine mesh was chosen in the FE model. A second-order fit $L_1(x) = L_0 + \alpha_1(x - x_{so}) + \alpha_2(x - x_{so})^2$ was obtained by minimizing the RMS deviations between the model results and the fit. L_0, α_1 and α_2 were obtained as 35 nH, $4.49{\cdot}10^{-4}$ H/m and -0.96 H/m^2, respectively.

2.2. Interface behavioral model

The behavior of the interface, illustrated in Fig. 1(a), is modelled in MATLAB. The oscillator amplitude is evaluated as $|V_o| = 2\pi{\cdot}f_{osc}{\cdot}L{\cdot}I_{LC}$ where f_{osc}, L and I_{LC} are: oscillation frequency, coil inductance and tank-resonance current, respectively. Oscillator amplitude can drift over time due to drift of any of these quantities and can manifest itself as a change in inductance after demodulation. Hence, ratio-metric measurement is required to suppress these effects and guarantee a stable ECDS system [3].

The nonlinear behavior of the interface is modelled as $V_{out} = \beta_1 V_o + \beta_2 V_o^2$. The interface is assumed to be limited by 2nd order nonlinearity due to pseudo-differential sensor architecture. For a given total drift-budget (e.g. 1 %), the largest value of β_2/β_1 is evaluated such that the maximum error in D_{out} stays below 1 *LSB*, which is equal to 105 pm, for $x_{so} = 55$ μm and 19 bits accuracy.

3. Stability and nonlinearity

Figure 3(a) shows the transfer characteristics of the sensor coil and the variation in oscillation frequency due to inductance change, over 5 μm displacement range around $x_{so} = 55$ μm. The nominal oscillation frequency is 200 MHz, which is required to reduce skin depth to 4.7 μm (for Cu target) to enable sub-nanometer displacement sensing. The nominal value of sensor inductance is 35 nH.

Figure 3(b) depicts errors in D_{out} due to the sensor nonlinearity, interface nonlinearity and drift, for $|\beta 2/\beta 1| = 2{\cdot}10^{-3}$, when compared to a linear sensor ($L_1(x)$ with $\alpha_2 = 0$). The additional error incurred due to the interface nonlinearity (difference between blue and black curves) is much smaller than the absolute error caused by the sensor nonlinearity (blue curve), hence the performance is limited by the sensor.

Fig. 3(b) also shows the excess error in D_{out}, caused by 1 % drift in the oscillator amplitude, which remains under 1 *LSB*. The drift is assumed to be caused by any of the entity which defines the oscillator output amplitude (as discussed in Section 2.2). For 250 mV oscillator output amplitude and $|\beta_2/\beta_1| = 2{\cdot}10^{-3}$, the maximum interface nonlinearity that can be tolerated evaluates to −72 dB HD2. The sensor nonlinearity is −51.5 dB for 5 μm displacement around $x_{so} = 55$ μm (Section 2.1).

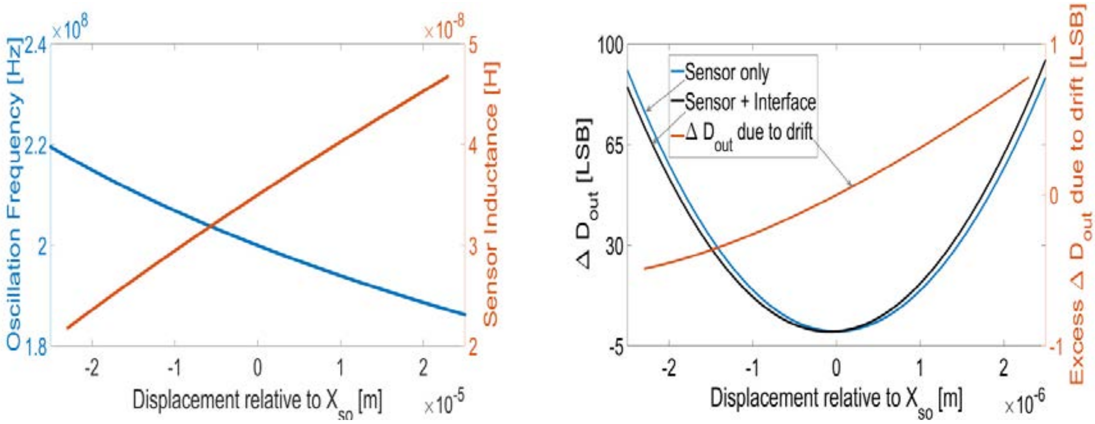

(a) (b)

Fig. 3. (a) Oscillation frequency and Sensor inductance as a function of displacement relative to standoff of 55 μm. (b) Errors in the ratiometric read-out vs. displacement due to sensor nonlinearity, interface nonlinearity and drift, compared to a linear sensor.

4. Summary

We investigated the suppression efficiency of ratiometric readout, in presence of sensor nonlinearity and interface nonlinearity, in a pseudo-differential eddy-current displacement sensor (ECDS). We utilized FE model to characterize the sensor coil and MATLAB to model nonlinear behavior of the interface. It is found that, in order to tolerate 1 % drift in the oscillator amplitude, a maximum 2nd harmonic distortion (HD2) of the interface has to be less than −72 dB when the sensor HD2 is −51.5 dB for 5 μm displacement around x_{so} = 55 μm. For a more stable ECDS system, even higher linearity is required from the interface.

Acknowledgements

Authors would like to thank Dutch funding agency STW for its support for this research and Mohammad Nabavi for useful discussions.

References

[1] S. Nihtianov, "Measuring in the Sub-nanometer Range: Capacitive and Eddy Current Nano-displacement Sensors", Industrial Electronics Magazine, IEEE, vol. 8, no. 1, pp. 6-15, 2014.
[2] "Eddy Current Sensors for Displacement and Position DT3703", Data Sheets. Micro-Epsilon, 2012 [Online]: www.micro-epsilon.com
[3] S. D. Roach, "Designing and building an eddy current position sensor," *Sensors*, vol. 15, no. 9, 1998.
[4] M. R. Nabavi and S. N. Nihtianov, "Design strategies for eddy-current displacement sensor systems: Review and recommendations", IEEE Sensors J., vol. 12, no. 12, pp. 3346-3355, 2012.
[5] M. R. Nabavi, M. A. P. Pertijs, and S. Nihtianov, "An Interface for Eddy-Current Displacement Sensors With 15-bit Resolution and 20 MHz Excitation," J. Solid-State Circuits, vol. 48, no. 11, pp. 2868–2881, 2013.
[6] G. Tian, Z. Zhao, and R. Baines, "The research of inhomogeneity in eddy-current sensors," Sensors and Actuators A: physical, vol. 69, no. 2, pp. 148–151, 1998.